

The Unusual Intensity Pattern of OH(6,2) and O(1S) Airglow Observed Over the Andes Lidar Observatory

Tai-Yin Huang*, Yolián Amaro-Rivera, Fabio Vargas, and Julio Urbina

**Physics Department*
Penn State Lehigh Valley



AS1.34, EGU, Vienna, Austria, May 7, 2020



Introduction

- Simultaneous OH(6,2) and O(¹S) nightglow measurements at the Andes Lidar Observatory (ALO) (30.3°S, 70.7°W) from September 2011 to April 2018 have been analyzed to investigate an unusual intensity pattern, that is, O(¹S) nightglow intensity enhancement concurrent with OH(6,2) nightglow intensity weakening.
- We have identified 142 nights showing that behavior during the time period.
- A semidiurnal tide fitting applied to the 30-min bin size monthly averaged data shows that the largest amplitudes of the tide occur in April-May and August-September in both OH(6,2) and O(¹S).

Introduction...Continued

- SABER atomic oxygen (O) climatology near ALO shows higher O densities near the equinoxes, with maximum O densities in March and September at ~96 km.
- Lidar temperature analysis suggests that the O(¹S) enhancement concurrent with the OH(6,2) weakening is often accompanied by a temperature increase at 96 km and a decrease at 87 km.
- Simulations using two airglow models, OHCD and MACD, have also been carried out to investigate the effect of a semidiurnal tide on the OH(6,2) and O(¹S) airglow intensities.
- A sensitivity study has also been conducted to illustrate the effect of the characteristics of the semidiurnal tide on the airglow intensity patterns.

Key Findings

- O(¹S) enhancement concurrent with OH(6,2) weakening is often accompanied by a temperature increase at 96 km and a temperature decrease at 87 km
- Simulation results illustrate how the combination of factors (larger tidal amplitudes, temperature gradient, and greater amount of [O]) can produce the unusual intensity pattern observed in the airglow data
- The characteristics of the semidiurnal tide play a major role in the O(¹S) and OH(6,2) intensity patterns

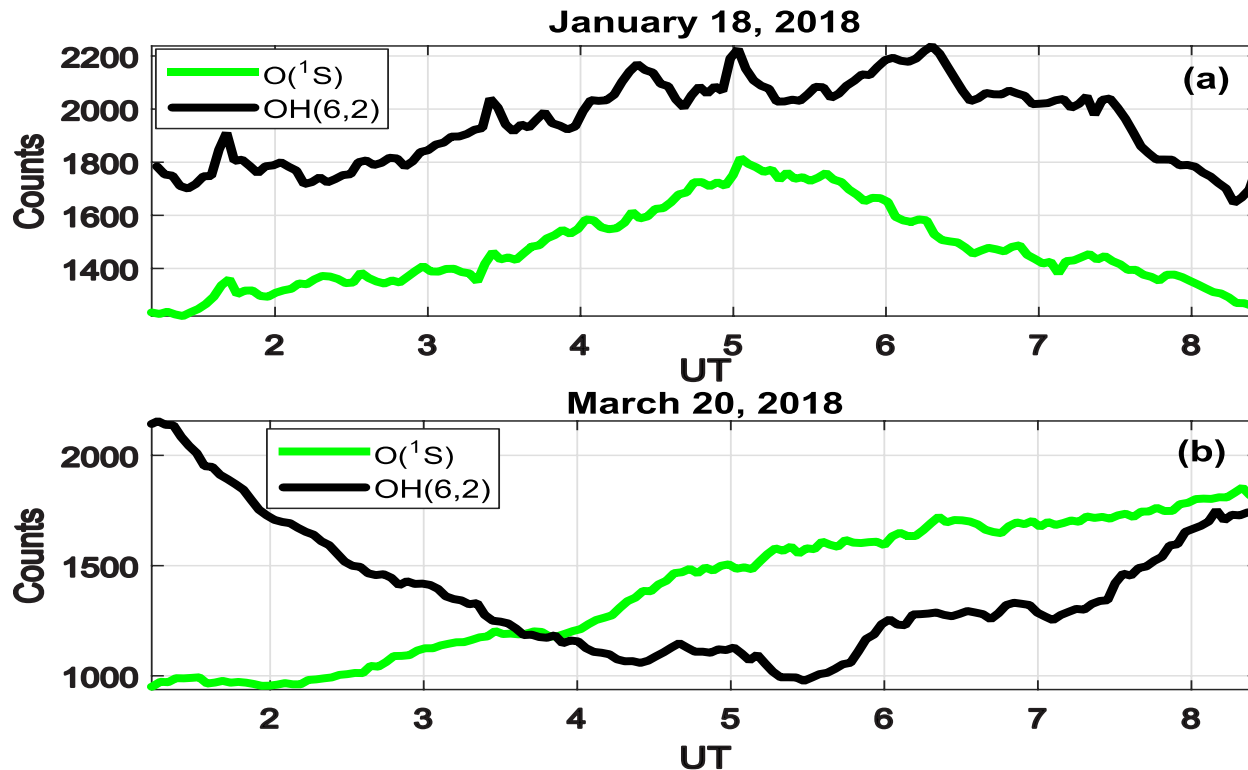
Observations used in the study

The data was collected during September 2011 - April 2018 near the Andes Lidar Observatory (ALO) (30.3°S , 70.7°W) in Chile



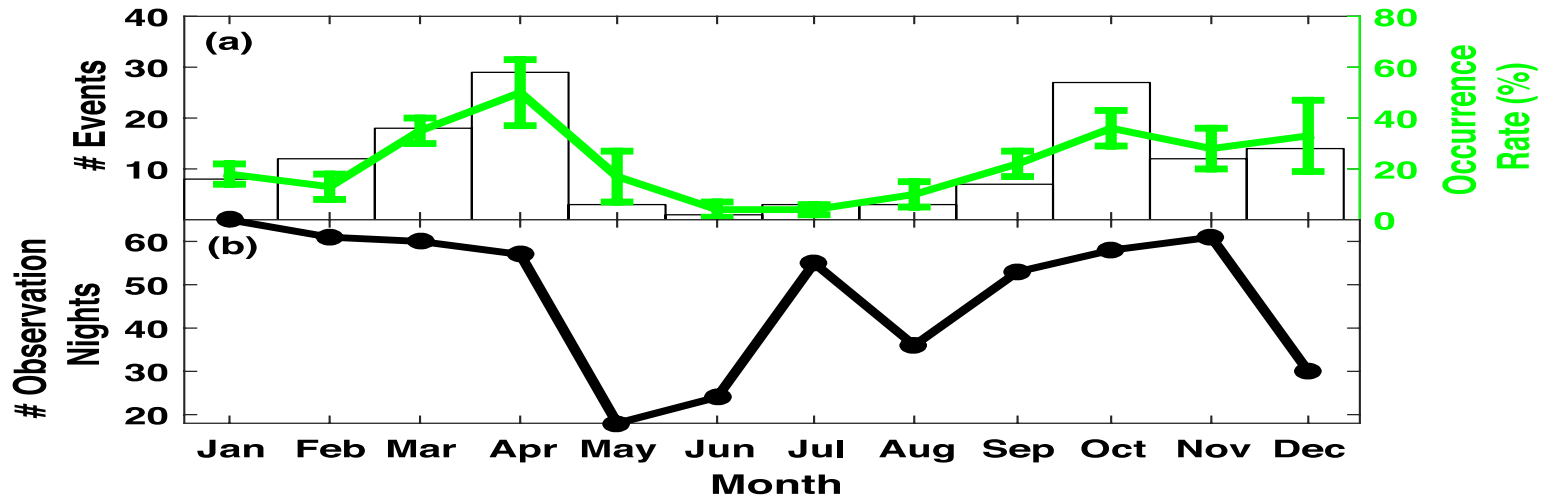
- The **OH(6,2)** and **O(¹S)** airglow **data** were collected with a CCD imager.
- The **temperature** data was obtained with a Na lidar system.
- The lidar measures Na density, temperature, and wind between 80 km and 110 km with a temporal resolution of ~ 1 min and a vertical spatial resolution of 500 m.
- The **O densities** were obtained from SABER near the ALO location

Unusual Intensity Pattern Observed by a CCD imager at Andes Lidar Observatory (ALO)

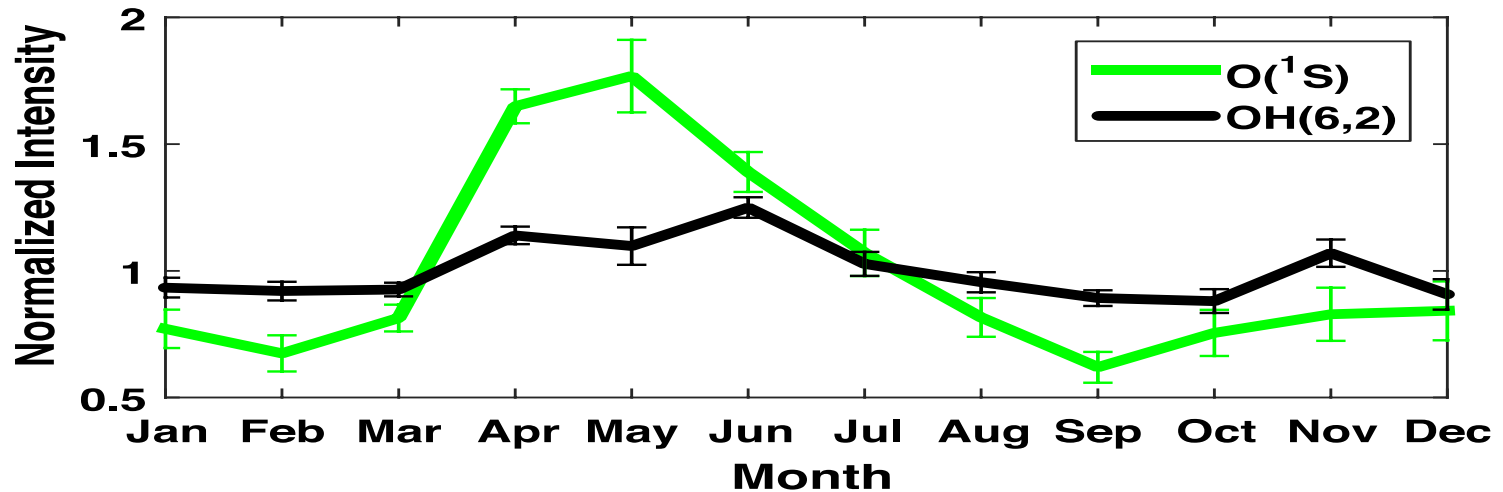


(a) Example of a typical $OH(6,2)$ and $O(^1S)$ intensity pattern.

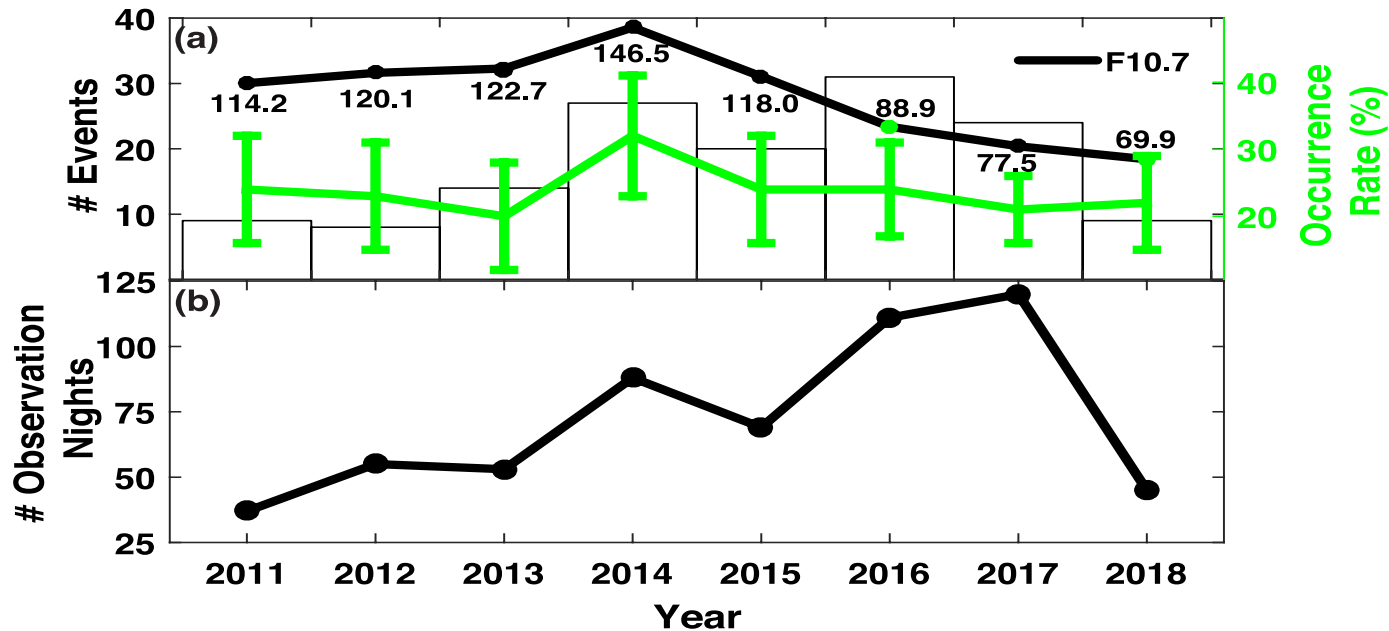
(b) Example of an unusual $OH(6,2)$ and $O(^1S)$ intensity pattern. $O(^1S)$ gets enhanced while $OH(6,2)$ gets weaker during ~2:00 to ~4:20 UT.



(a) Monthly distribution of the unusual patterns and occurrence rate (%).
 (b) Number of observation nights by month.



Monthly average of normalized intensities from the 2011-2018 period.



(a) Annual distribution of the unusual pattern, F10.7 solar flux, and occurrence rate (%).

(b) Number of observation nights per year.

The events have a yearly occurrence rate of ~24%. A higher occurrence rate (32%) is observed for the year 2014

The 2014 solar maxima might have contributed to the larger occurrence rate of the events recorded for the same year due to the increase of [O] in the mesosphere.

Table 1. Monthly and annual distribution of the OH(6,2) and O(¹S) unusual intensity pattern events.

	2011	2012	2013	2014	2015	2016	2017	2018	Total
Jan		0	0	3	3	0	3	2	11
Feb		0	0	0	2	4	3	0	9
Mar		2	4	4	1	2	2	3	18
Apr		0	6	8	11	0	0	4	29
May		0	0	2	1	0	0		3
Jun		0	0	0	0	1	0		1
Jul		2	0	0	1	0	0		3
Aug		0	0	0	0	3	1		4
Sep	1	0	1	5	0	1	3		11
Oct	5	1	3	5	0	5	5		24
Nov	3	2	0	0	1	5	4		15
Dec	0	1	0	0	0	10	3		14
Total	9	8	14	27	20	31	24	9	142

There were 29 instances in which events were detected during consecutive nights. The groups of consecutive nights with the largest number of occurrences were April 20 - 26, 2015 (7 nights), December 1 - 5, 2016 (5 nights), and December 26 - 30, 2016 (5 nights).

Fitting With a Semidiurnal Tide

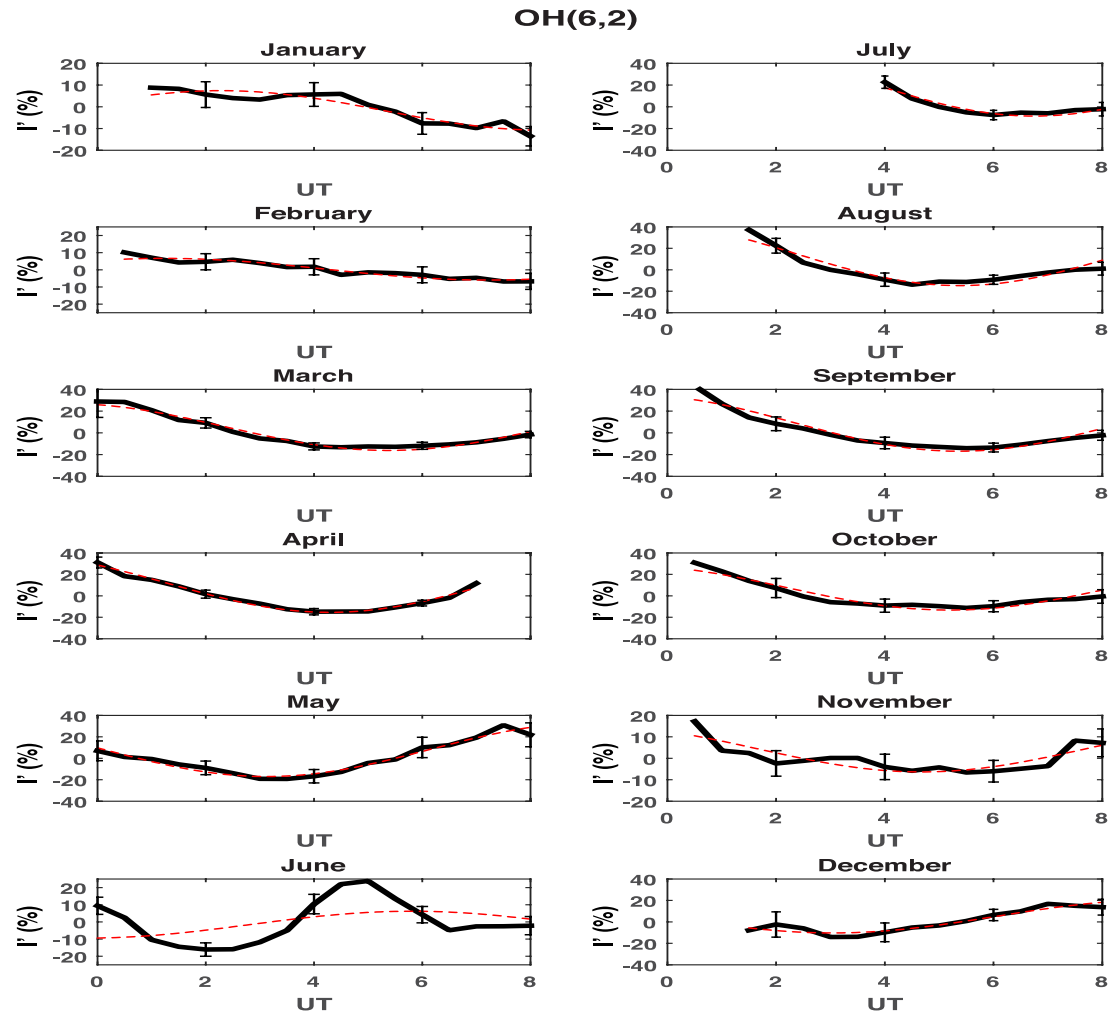
We fit the data with a semidiurnal tide to identify any tidal wave characteristics. The amplitudes and phases of the semidiurnal tide are obtained by applying a least square fit to the data using

$$I(t) = \bar{I} + \hat{I} \cos[2\pi(t - \theta)/\tau]$$

where \bar{I} is the 30-min binned monthly mean intensity (counts), \hat{I} is the amplitude (counts), τ is the period (in hours), t represents time (in hours), and θ is the phase (in hours).

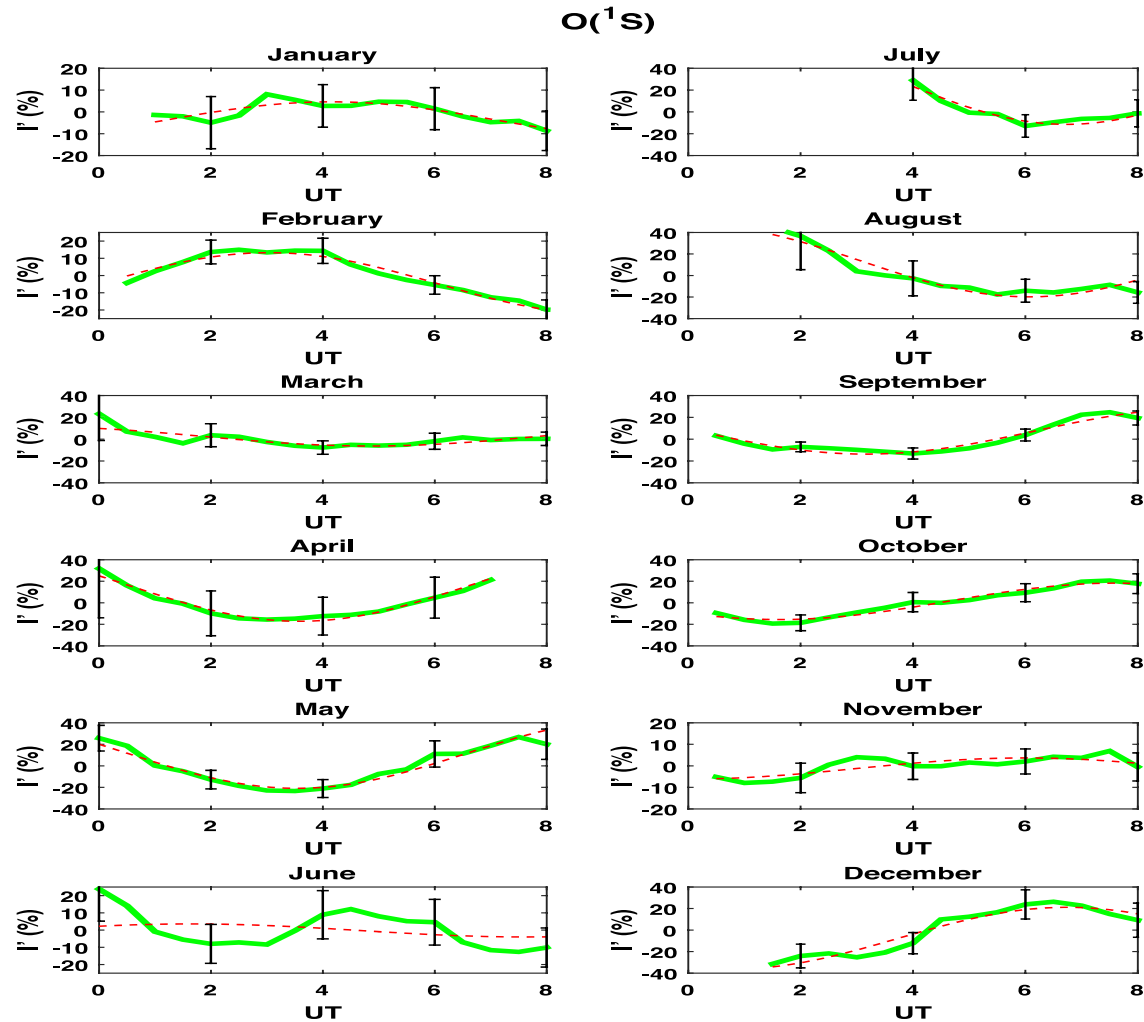
It should be noted that the imager can only resolve waves with the vertical wavelengths larger than the width of the airglow layer.

Semidiurnal Tidal Fitting (red dotted line) and OH(6,2) Data



The semidiurnal tide fits the data very well for most of the months except for June.

Semidiurnal Tidal Fitting (red dotted line) and O(1S) Data



The semidiurnal tide also fits the data very well for most of the months except for June.

Table 2. Semidiurnal amplitudes and phases from the fitting. Phases are in reference to midnight (0 UT).

	OH(6,2)				O(¹ S)			
	Ampl (counts)	Ampl (%)	Phase (h)	R ²	Ampl (counts)	Ampl (%)	Phase (h)	R ²
Jan	136.92	7.42	2.28	0.8815	37.558	4.61	4.15	0.7177
Feb	123.85	6.63	1.22	0.9025	95.942	13.31	3.03	0.9669
Mar	504.16	25.66	-0.63	0.9613	83.602	9.77	-1.14	0.5637
Apr	578.08	28.32	-1.71	0.9786	425.57	24.66	-2.42	0.9613
May	634.00	28.53	-2.87	0.9532	612.91	32.76	-2.46	0.9238
Jun	147.94	6.22	-0.19	0.2060	50.842	3.55	1.64	0.0854
Jul	306.13	17.34	0.75	0.8763	214.69	22.94	0.73	0.8873
Aug	514.82	27.46	-0.62	0.8870	295.36	37.64	0.07	0.9189
Sep	549.92	30.11	-0.64	0.9152	154.16	24.47	-2.84	0.9276
Oct	414.18	23.63	-0.80	0.9125	134.56	18.21	-4.38	0.9607
Nov	234.43	10.42	-1.32	0.6940	32.552	3.67	-6.01	0.6163
Dec	328.86	18.16	-2.96	0.9130	169.66	21.26	-5.26	0.9283

The semidiurnal tidal fitting in June does not adequately describe the data as indicated by the low R² values

The OHCD and MACD Model Simulations

The SABER [O] profiles used as input to the OHCD and MACD models were perturbed with a vertical oscillation and are described by

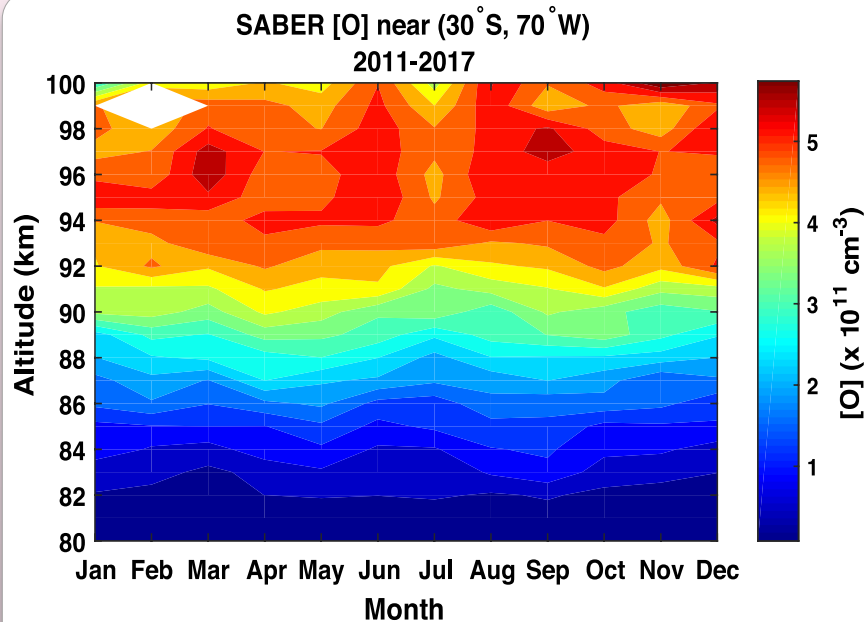
$$[O] = \overline{[O]} + [\widehat{O}] e^{\frac{z}{2H}} \cos\left(\frac{2\pi}{\tau} t - \frac{2\pi}{\lambda_z} z + \theta\right)$$

where $\overline{[O]}$ is the original density profile, $[\widehat{O}]$ is the initial amplitude perturbation, H is the atmospheric density scale height, τ is the wave period, λ_z is the vertical wavelength (km), and θ is the phase (rad).

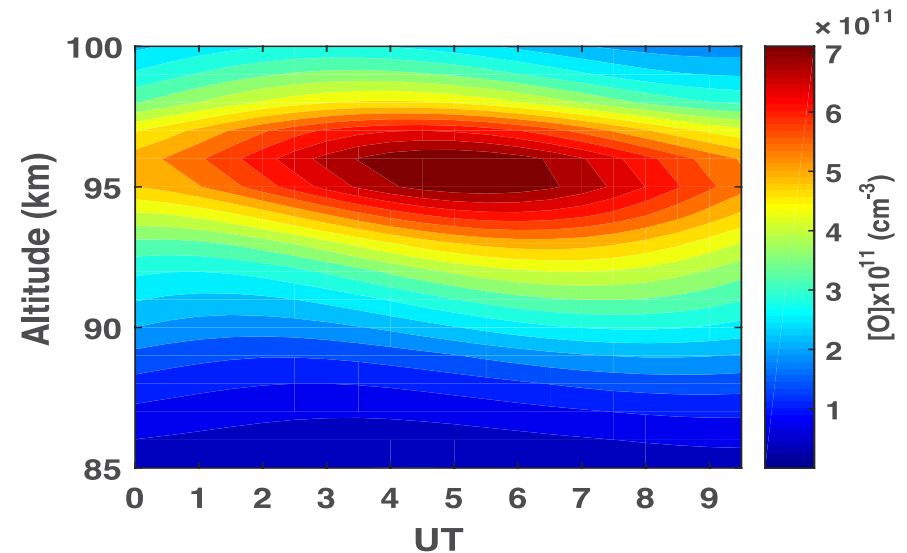
The amplitudes and phases used in the simulations were obtained from the 12-h fittings applied to the nightly intensity time series.

The OHCD model chemistry involves six species (O, O₃, H, HO₂, OH(v=0), and OH*(v')) (Huang and Hickey (2007; 2012)), with reaction rates and Einstein coefficients adjusted for the OH(6,2).

The MACD model includes five species (O, O₂(c¹), O₂(0,0), O₂(0,1), and O(1S)) (Huang and George, 2014), with updated branching ratios as described by Amaro-Rivera et al. (2018).



SABER monthly mean of [O] at latitude 30°S ±10° and longitude 70°W±10° for 2011-2017.



SABER O densities perturbed by a 12-h period wave with a vertical wavelength of 35 km, amplitude of 35%, phase of 90°. The initial profile was obtained near ALO for November 7, 2015 at ~1 UT.

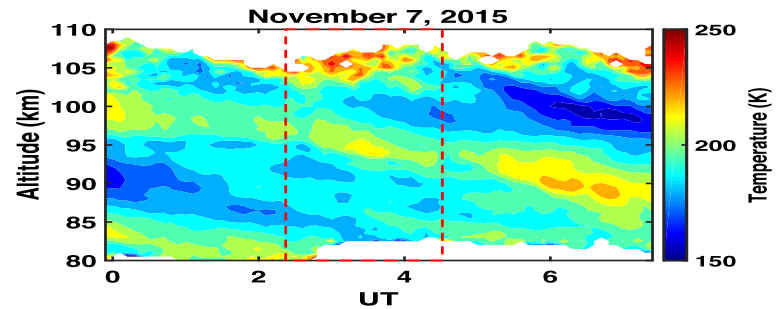
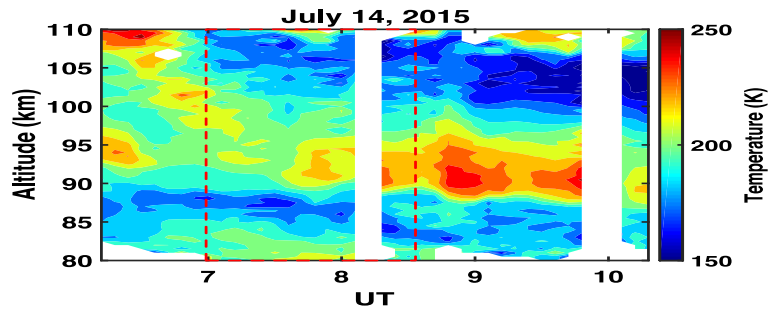
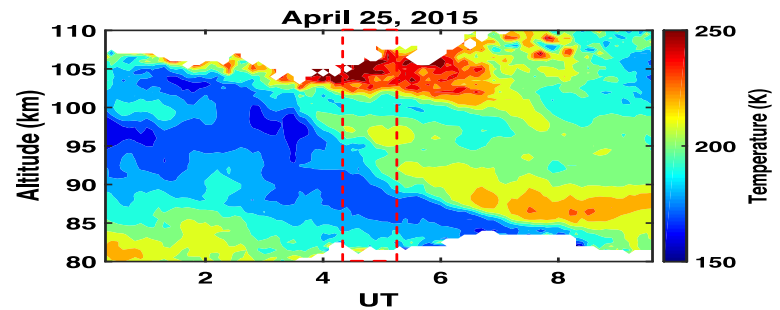
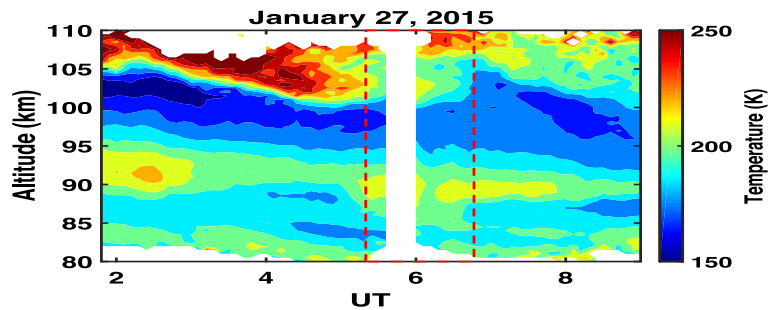
SABER O densities for the following nights were input to the airglow models.

January 27, 2015 (30.1°S, 71.5°W, 0:59:41 UT, event 59)

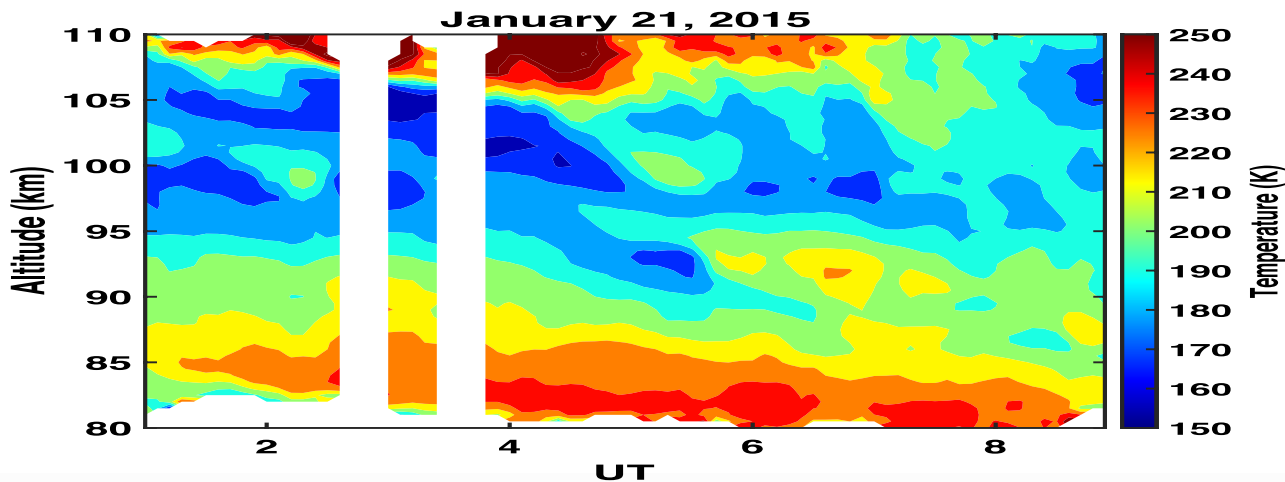
April 25, 2015 (31.0°S, 74.5°W, 1:49:45 UT, event 56)

July 14, 2015 (35.1°S, 74.2°W, 1:22:34 UT, orbit 88)

November 7, 2015 (28.7°S, 71.6°W, 0:35:41 UT, event 81).

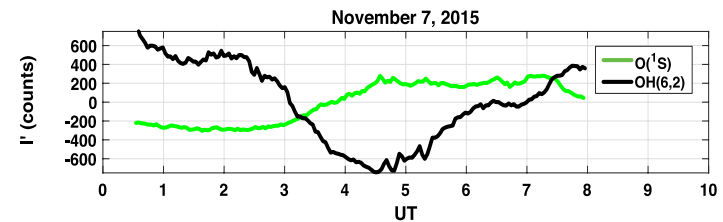
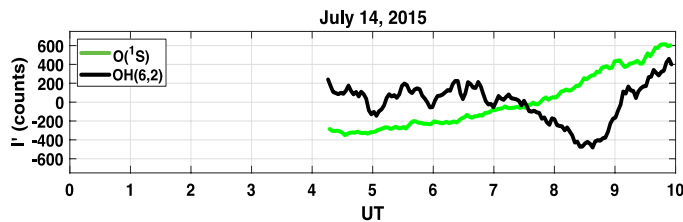
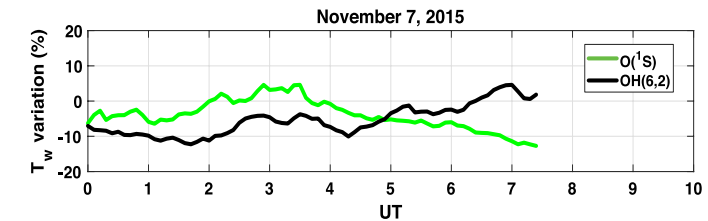
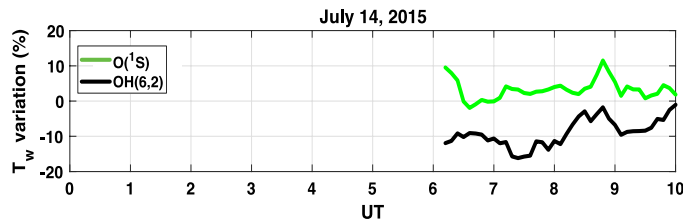
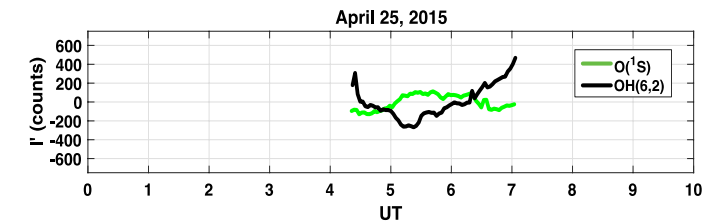
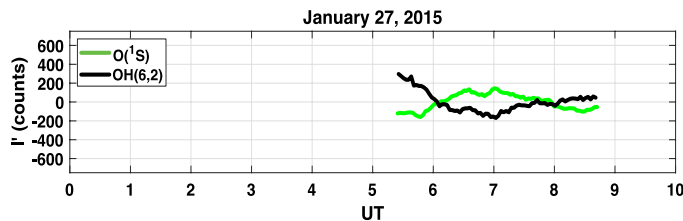
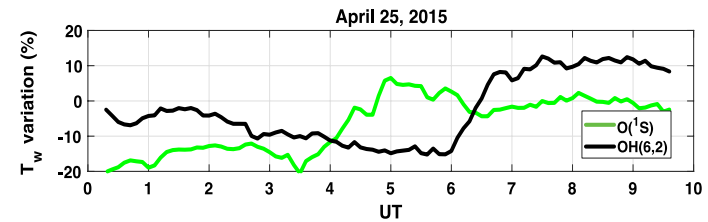
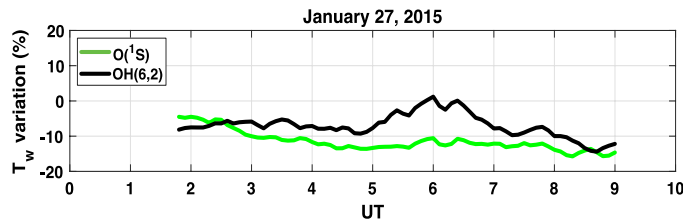


Na lidar temperatures at ALO for the selected nights. The dotted box indicates the time period in which the events were observed.

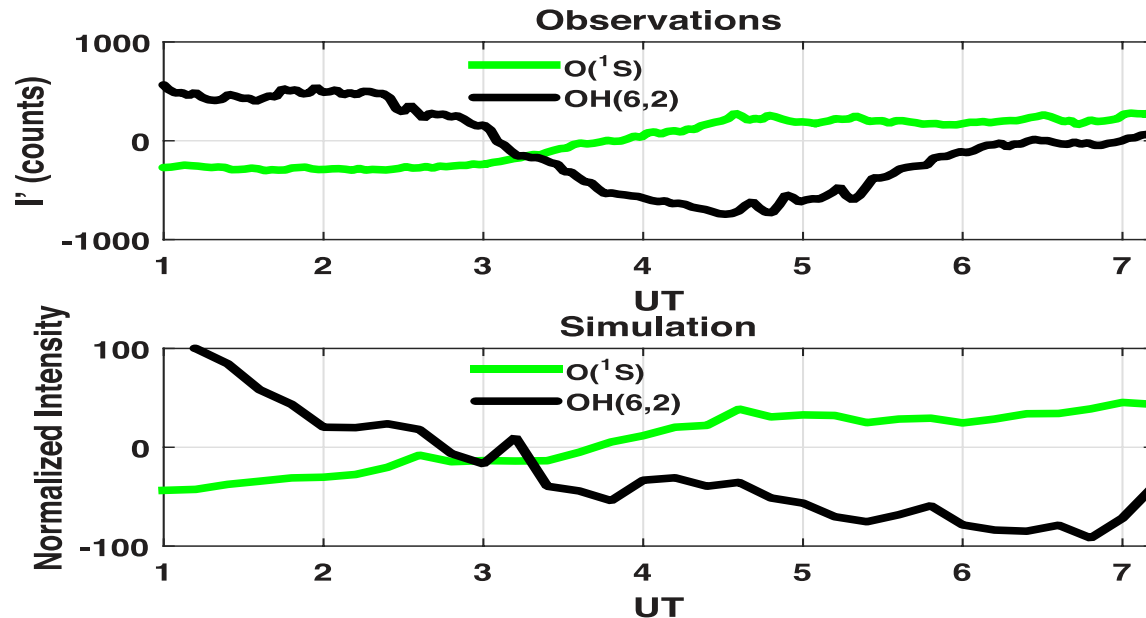


Na lidar temperatures for a typical night.

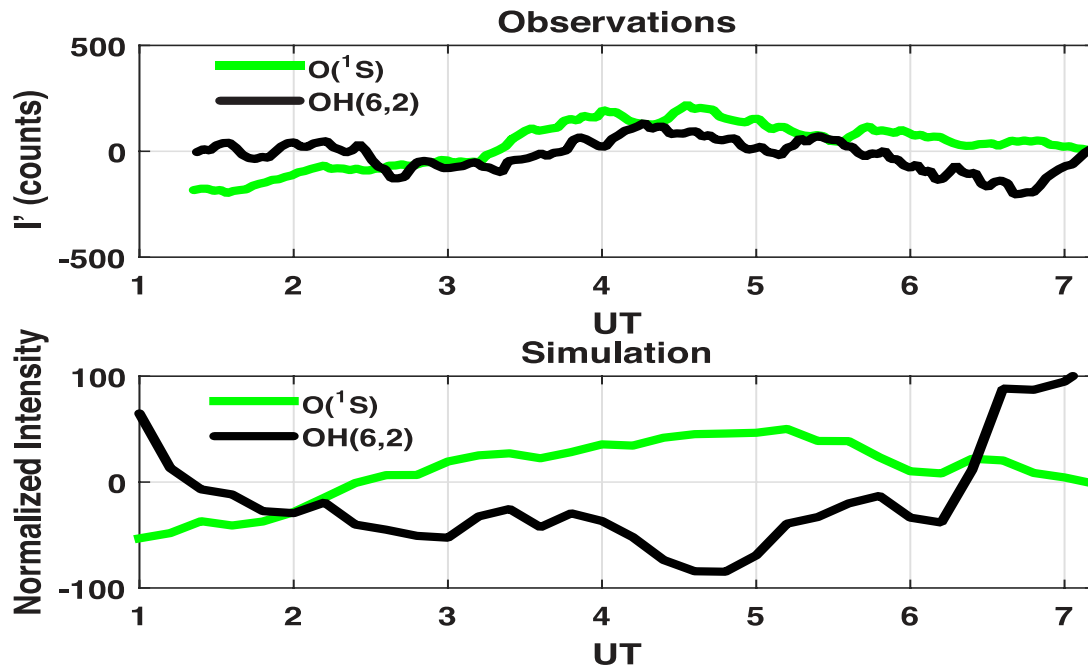
Simulated Intensity-weighted temperature Variations and Intensities



Lidar temperatures and the SABER [O] densities were input to the OHCD and MACD to get the intensity-weighted temperature variations and intensities. The 3 of the 4 events displayed a temperature increase at 96 km and a decrease at 87 km.

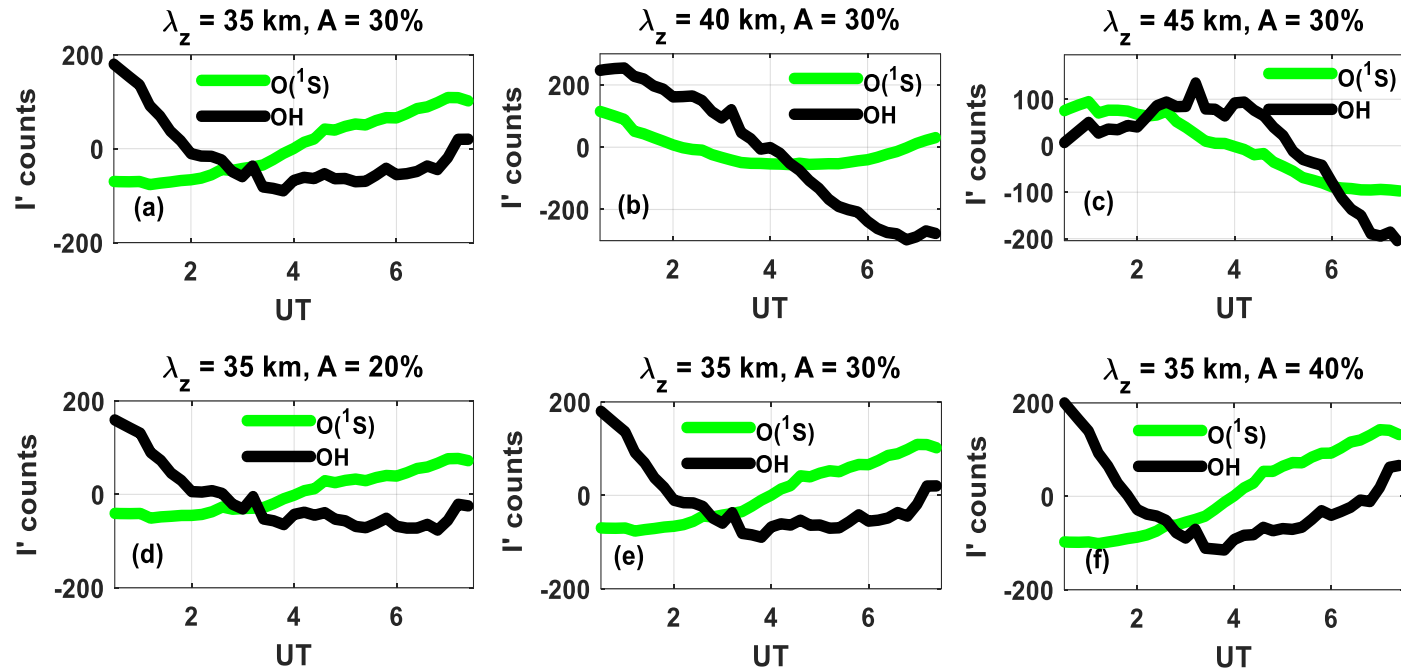


- OH(6,2) and O(¹S) normalized airglow intensities obtained from the ALO CCD imager on Nov. 7, 2015..
- OH(6,2) and O(¹S) normalized airglow intensities simulated with the OHCD and MACD models. The temperature profiles from the Lidar and perturbed SABER O densities are input to the models to simulate the normalized intensities.
- The simulation shows good agreement with the observation for the unusual intensity pattern when the semidiurnal tide is used.



- $OH(6,2)$ and $O(^1S)$ normalized airglow intensities obtained from the ALO CCD imager for January 21, 2015.
- $OH(6,2)$ and $O(^1S)$ normalized airglow intensities simulated with the OHCD and MACD models. The temperature profiles and perturbed SABER O were used as input to the models.
- $[O]$ is perturbed by a semidiurnal tide with a vertical wavelength of 35 km, amplitude of 12%, and a 30° phase.
- The simulation illustrates that a semidiurnal tide alone does not reproduce the pattern for a typical night for the OH intensity.

Simulated O(¹S) and OH(6,2) airglow intensities



- The O densities are perturbed with a semidiurnal tide with different vertical wavelengths (λ_z) and amplitudes (A).
- The vertical wavelength has a significant effect on the intensity patterns.
- The tidal amplitude also plays a role on the patterns, with the larger amplitude causing a steeper increase in the intensities.

Summary

- Events of increasing O(¹S) intensity concurrent with OH(6,2) intensity weakening from Sept. 2011 to April 2018 were analyzed.
- Occurrence rate of the events was characterized was found to be ~24% with a higher occurrence rate for 2014 (32%), which coincides with the solar max of cycle #24.
- O(¹S) enhancement concurrent with OH(6,2) weakening is often accompanied by a temperature increase at 96 km and a temperature decrease at 87 km.
- A semidiurnal tidal fitting to the monthly mean intensity data shows that it fits the intensities very well except for the month of June.
- SABER [O] densities and ALO Lidar temperatures were input to the OHCD and MACD models with the [O] perturbed by the semidiurnal tide identified from the data.
- The model simulations indicate that the events can be reproduced rather well.